

ARTICLE

Low-density superhard materials: Computational study of Li-inserted B-substituted closo-carboranes LiBC₁₁ and Li₂B₂C₁₀

Received xxth xx 20xx,
Accepted xxthxx 20xx

DOI: 10.1039/x0xx00000x

www.rsc.org/

Xiaolei Feng^a, Xinyu Zhang^a, Hanyu Liu^b, Xin Qu^{cd}, Simon A. T. Redfern^e, John S. Tse^{*ab}, and Quan Li^{*a}

Insertion of Li atoms into a B-substituted carbon cage produces two superhard compounds with relatively low density: LiBC₁₁ and Li₂B₂C₁₀. For each structure, phonon frequencies across the whole Brillouin zone are positive, indicating dynamical stability. Electronic structure calculations indicate that they are semiconductors under ambient conditions. Estimates of the Vickers hardness, based on a semi-empirical model, highlight the incompressible nature of these two compounds. We then performed calculations on the ideal strengths of these two structures to confirm the hardness and investigate origins of the mechanical properties. Strikingly, both LiBC₁₁ and Li₂B₂C₁₀ can be classed as superhard materials, with hardness of 49 GPa and 41 GPa, respectively. The current results shed light on the properties of new superhard carbon cage structures more generally.

Introduction

The search for superhard materials with Vickers hardness, $H_v \geq 40$ GPa has been an important focus for some time in materials science and technology. A well-known family of superhard materials is that comprising light elements compounds (such as C₃N¹, B₂CO², BC₂N^{3,4}, B₃NO⁵, diamond, BC₃^{6,7}, BC₅^{8,9}, BC₇¹⁰, B₆O¹¹, *pnnm*-CN¹², CN₂¹³, BC₂N^{14,15}, and *c*-BN¹⁶), where strong covalent bonding between light elements often leads to the formation of rigid three-dimensional crystalline networks with extreme resistance against stresses across a wide range of loading conditions. The low thermal stability of diamond in oxidizing environments and the high synthetic cost of these traditional superhard materials, have stimulated the search for novel superhard materials exhibiting improved stability over a wide range of conditions with good properties.

Sodalite-like cages (named after the cage zeolitic oxide) formed by groups of 12 atoms are thought to be the root of some extraordinary properties. A good example is a new clathrate sodalite-like structure of BN, which has recently been predicted to be “superhard”, with a hardness of 58.4 GPa¹⁷. Considering the important role carbon plays in the materials world, it is interesting to explore the effects of inserting metal atoms into sodalite-like C cages. With larger atomic radii, C cages display relatively smaller cavities, even for the smallest metal atom (we consider Li atoms in this work). This inevitably leads to structural destabilization: here

we seek to explain the electronic origins of such destabilization. Since a closed-shell electron configuration is helpful to stabilise a compound, and the C atoms forming the cages form already have a closed-shell electronic configuration, the insertion of electropositive Li atoms donate electrons to the antibonding bands and weaken the bonding. **The insertion of Li does not, of itself, lead to superior hardness, but it does stabilise superhard phases.** It is necessary to maintain the strong chemical bonds by adjusting the number of electrons in the system. One possible solution is to substitute C atoms with electron deficient B atoms in the framework as proposed by Tao Zeng *et al.* in their recent work¹⁸. In fact, isolated closo-carboranes, like 1,5-C₂B₃H₅, 1,6-C₂B₄H₆, 2,4-C₂B₅H₇, have been synthesised experimentally¹⁹, therefore there is a good possibility that the bulk solid closo-carboranes may also be synthesised.

We explored the possibility of stabilizing the sodalite-like C cage by two strategies of coupled Li-insertion – B-substitution and proposed two compounds (LiBC₁₁ and Li₂B₂C₁₀), stable at ambient conditions. Electronic structure calculations suggest that both compounds are semiconductors with band gaps of 0.6–1.3 eV. Subsequent first-principles study of their mechanical properties indicates that both compounds are superhard. Moreover, they are also the lightest compounds among the family of known light element superhard materials. The predicted stable, superhard, Li/B/C ternary compounds, with remarkably low density, may have great potential importance for technological application and shed light on the general principles on the rational design of superhard structures.

^aState Key Laboratory of Superhard Materials and College of Materials Science and Engineering, Jilin University, Changchun, 130012, China.
E-mail: liquan777@jlu.edu.cn

^bDepartment of Physics and Engineering Physics, University of Saskatchewan, Saskatoon, Saskatchewan S7N 5E2, Canada E-mail: john.tse@usask.ca

^cChangchun Institute of Optics, Fine Mechanics and Physics, Chinese Academy of Sciences, Changchun 130033, P. R. China

^dUniversity of Chinese Academy of Sciences, Beijing 100039, P. R. China

^eDepartment of Earth Sciences, University of Cambridge, Cambridge, CB2 3EQ, UK

Computational methods

First-principles electronic structure calculations were based on density functional theory (DFT) and performed using the Vienna *ab initio* simulation package (VASP)²⁰. The generalised gradient approximation (GGA) in the scheme of Perdew-Burke-Ernzerh of (PBE)²¹ was used to describe the electron exchange correlation

interactions, while electron-ion interactions were treated using projected-augmented-wave (PAW) potentials²². PAW potentials with $1s^22s^1$, $2s^22p^1$, and $2s^22p^2$ electrons as valence electrons were adopted for the Li, B, and C atoms, respectively. A kinetic-energy cutoff of 720 eV and Monkhorst-Pack²³ meshes for Brillouin Zone sampling with a resolution of 0.01 \AA^{-1} were chosen. The atomic relaxation was terminated when the change in the total energy per atom converged to less than 1 meV. To confirm the dynamical stability of the structures, we computed the phonon dispersions using a supercell approach as implemented in PHONOPY code^{24, 25} with $2 \times 2 \times 2$ supercells. Elastic constants were computed from the strain-stress method, and the bulk and shear moduli were thus derived from the Voigt-Reuss-Hill averaging scheme²⁶. The Vickers hardness was first estimated from a semi-empirical microscopic hardness model²⁷. The exact stress-strain relation was then obtained explicitly by calculating the stress response to structural deformation along specific loading paths using a quasi-static relaxation method. The latter method can simulate various loading conditions and determine the corresponding ideal strength and deformation modes²⁸⁻³¹.

Results and discussion

The sodalite-like carbon cage adopts a remarkable cubic configuration ($Im\bar{3}m$, Pearson symbol cI14), with all 12 carbon atoms sharing identical point symmetry (Fig. 1(c)). The calculated cubic cell parameter is in good agreement with the hypothetical structure proposed by *Filipe et al.*³². The small difference (0.98%) between our calculated cubic unit cell lattice parameter and that of *Filipe et al.*³² can be explained by the different electron exchange correlation interactions chosen (PBE in this work and LDA in Ref. 32). To maintain the total number of electrons after inserting a Li atom into the cavity, we replaced one of the framework C atoms with a B and then the structure was fully re-optimised. The resulting LiBC_{11} maintains the framework topology although the cage is slightly deformed. We further placed two Li atoms into two cavities formed by a double B-substituted C cage. In this case, there are five distinct ways for the double B substitutions. We examined all the possibilities and found that the most energetically favourable structure is to replace two non-adjacent atoms of one C-C bond. This configuration is in agreement with a previous study¹⁸. The unit cells of the resulting LiBC_{11} and $\text{Li}_2\text{B}_2\text{C}_{10}$ (lowest enthalpy) structures are shown in Fig. 1, and the corresponding equilibrium structural parameters and space group at ambient pressure are listed in Table 1. The bond length of B-C is 1.63 \AA and C-C bond lengths range from 1.55 \AA to 1.60 \AA in LiBC_{11} . In $\text{Li}_2\text{B}_2\text{C}_{10}$, the B-C bond length is 1.65 \AA while C-C bond lengths are $1.57/1.59 \text{ \AA}$.

Table 1 The space group and calculated equilibrium structural parameters: cubic unit cell parameters and Wychoff positions of LiBC_{11} and $\text{Li}_2\text{B}_2\text{C}_{10}$ at ambient pressure.

Phase	Space group	Lattice parameter (\AA)	Atomic coordinates (r/a, fractional)
C_{12}	$Im\bar{3}m$	$a=4.383$ $a=4.34^{\text{Ref 32}}$	C 12d(0.000,0.250,0.500)
LiBC_{11}	$Pmm2$	$a=4.470$ $b=4.469$ $c=4.441$	Li 1a (0.000, 0.000, 0.058) B 1c (0.500, 0.000, 0.249) C 2e (0.240, 0.000, 0.504) C 2g (0.000, 0.251, 0.504) C 2h (0.500, 0.257, 0.986) C 2f (0.250, 0.500, 0.988) C 1b (0.000, 0.500, 0.244) C 1b (0.000, 0.500, 0.745) C 1c (0.500, 0.000, 0.743)
$\text{Li}_2\text{B}_2\text{C}_{10}$	$P4_2/mmm$	$a=4.578$ $c=4.424$	Li 2d (0.250, 0.000, 0.000) B 2e (0.000, 0.000, 0.250) C 4m (0.500, 0.749, 0.500) C 2f (0.500, 0.500, 0.250) C 4j (0.734, 0.000, 0.000)

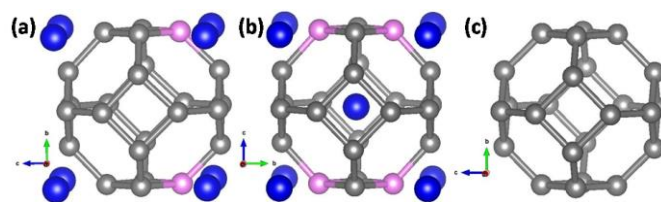


Fig. 1 (colour online) Crystal structures of (a) LiBC_{11} , (b) $\text{Li}_2\text{B}_2\text{C}_{10}$ and (c) C_{12} . The Li atoms are represented as large blue spheres, while B and C atoms are represented as small spheres, pink and grey respectively.

To investigate the electron structure, the valence band structures and the corresponding density of states projected onto the atomic orbitals (PDOS) were computed and the results are shown in Fig. 2. Here, the zero energy refers to the top of the valence band. LiBC_{11} and $\text{Li}_2\text{B}_2\text{C}_{10}$ are both semiconductors characterised by indirect band gaps of 1.3 eV and 0.6 eV, respectively. The HSE hybrid functional usually provides a better description of the electronic band structure^{33,34} (especially the band positions), but is computationally costly. In view of the fact that density functional theory, especially the semi-local PBE functional we used here, tends to underestimate the band gap of this class of compounds by 30% – 50%, we predict the experimental band gaps should be in the range of 1.9-2.6 eV and 0.9-1.2 eV for LiBC_{11} and $\text{Li}_2\text{B}_2\text{C}_{10}$, respectively. These values are considerably smaller than those of other light-element superhard materials (such as diamond, BC_3 , BC_5 , BC_2N , and cubic BN), which typically have band-gaps ranging from 3.0 eV to 3.6 eV. The small band gaps may suggest potential optical applications of these materials. A smaller gap is expected as an Li atom is introduced into the system since it will occupy the bottom of the conduction band. When a second B is inserted into the structure, the bottom of the conduction band [in Fig. 2(c)] is lowered, resulting an even lower band gap compared with that in Fig. 2(a). The PDOS plots demonstrate that C-2p electrons contribute most to both the upper conduction bands and lower valence bands.

The calculated electron localization functions show both LiBC_{11} and $\text{Li}_2\text{B}_2\text{C}_{10}$ are ionic with the Li atoms donating their valence electrons to the B such that the effective configuration of B becomes s^2p^2 , as for the carbon. The ionic LiBC_{11} and $\text{Li}_2\text{B}_2\text{C}_{10}$ compounds are isoelectronic with the C_{12} cage. Therefore, the strong covalent bonding between C-C and B-C are maintained thus preserving the stability of the rigid three-dimensional crystalline networks.

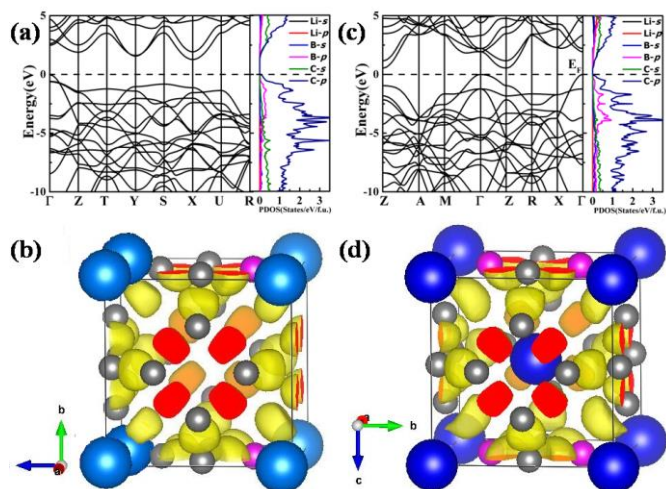


Fig. 2 (colour online) Calculated band structures and PDOS for (a) LiBC_{11} and (c) $\text{Li}_2\text{B}_2\text{C}_{10}$.

calculated electron localization function (isosurfaces=0.8) for (b) LiBC₁₁ and (d) Li₂B₂C₁₀, at 0 GPa.

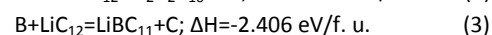
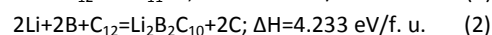
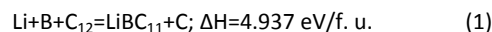
In Table 2, information on the calculated volume per unit cell, the volume per atom and the density of LiBC₁₁ and Li₂B₂C₁₀ are listed. Comparisons are made with the corresponding values for the empty C₁₂ cage structure and for several previously proposed light-element superhard materials. It can be seen that the cage structures display larger volumes than non-cage structures. Specifically, the volume of the unit cell of Li₂B₂C₁₀ (92.71 Å³) is substantially larger than that of LiBC₁₁ (88.71 Å³). The volume per atom (the volume per unit cell divided by the total number of atoms in the unit cell) shows the same trend as the volume per unit cell: 6.82 Å³/atom and 6.60 Å³/atom for caged LiBC₁₁ and Li₂B₂C₁₀, respectively, in contrast to smaller values (ranging from 5.68 to 6.00 Å³/atom) for other materials. The densities for LiBC₁₁ and Li₂B₂C₁₀ are 2.805 and 2.787 g/cm³, respectively. These values are much lower than the densities of other well-known superhard materials such as 3.510 g/cm³ for diamond, 3.483 g/cm³ for c-BN and 3.265 g/cm³ for BC₅. It is worth noting that even though Li₂B₂C₁₀ has a smaller volume per atom than LiBC₁₁, because the formula unit contains more light atoms, it is less dense than LiBC₁₁, making it the lightest superhard material reported. This property may be related to the unexpected and so-far unidentified hard and transparent carbon phase found in a rock sample with an estimated density of 2.5 g/cm³ from the Popigai impact crater in Russia³⁵.

Table 2 The calculated volume per unit cell, the volume per atom and density for LiBC₁₁, Li₂B₂C₁₀ and earlier proposed light elements superhard materials.

Structure	Volume (Å ³ /unit cell)	Volume (Å ³ /atom)	Density (g/cm ³)
C ₁₂	81.75	6.81	2.843
C ₁₂ ^{Ref 32}	82.08	6.84	2.928
LiBC ₁₁	88.71	6.82	2.805
Li ₂ B ₂ C ₁₀	92.71	6.62	2.787
Diamond	11.35	5.68	3.510
c-BN	11.83	5.92	3.483
BC ₅	36.02	6.00	3.265

The thermodynamic stability of the two Li-B-carbides with respect to the decomposition into the respective elements, can be quantified by the formation enthalpies of two different reaction routes. The positive reaction enthalpies of reactions (1) and (2) below indicate that LiBC₁₁ and Li₂B₂C₁₀ are thermodynamically metastable. Li-substitution, as expected, is highly endothermic, as seen in reactions (3) and (4). B-substitution helps to stabilise Li-insertion into the carbon cages. The successful synthesis of several

isolated closo-carboranes, like 1,5-C₂B₃H₅, 1,6-C₂B₄H₆, 2,4-C₂B₅H₇¹⁹, indicate that there is a good possibility that the bulk solid closo-carboranes can be also synthesised although there are experimental challenges to overcome the activation barriers. Nonetheless, the example of the existence of metastable diamond demonstrates that routes to the synthesis of these compounds may indeed be tractable.



The structural stability of both LiBC₁₁ and Li₂B₂C₁₀ has been investigated by calculations of their phonon band structures and elastic constants. As can be seen in Fig. 3, there are no imaginary phonons in the Brillouin zone for both LiBC₁₁ and Li₂B₂C₁₀, confirming their dynamical stability. Based on the mechanical stability criteria³⁶ of orthorhombic or tetragonal crystals (where combinations of elastic constants have to exceed or equal zero), the calculated elastic constants also indicate that both LiBC₁₁ and Li₂B₂C₁₀ are mechanically stable under ambient pressure.

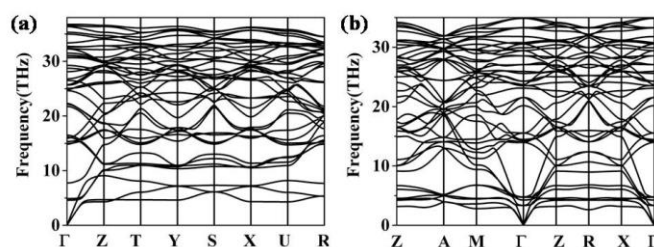


Fig. 3 (colour online) Calculated phonon dispersion curves for (a) LiBC₁₁ and (b) Li₂B₂C₁₀, at 0 GPa.

The mechanical hardness of a material is the ability to resist plastic deformation from hydrostatic compression, tensile load, and shear. Therefore, a superhard material usually requires a high bulk modulus (B_0) to resist volume decrease created by compression and also high shear modulus (G_0) to limit the creation and mobility of dislocations. In Table 3 we list the bulk and shear moduli of LiBC₁₁ and Li₂B₂C₁₀ derived from the calculated elastic constants. The calculated values for B_0 of LiBC₁₁ and Li₂B₂C₁₀ are 302 GPa and 208 GPa, and G_0 are calculated to be 271 GPa and 232 GPa, respectively, indicating the highly incompressible nature of these structures. We further estimated the Vickers hardness (H_v) using an empirical model²⁷ based on the correlation of the shear modulus with hardness. A comparison with the empty C₁₂ cage structure is listed in Table 3. High hardness values of 48.8 GPa and 37.7 GPa are estimated for LiBC₁₁ and Li₂B₂C₁₀, respectively. These values are slightly lower than that of the bare C₁₂ cage (51.5 GPa). To elucidate the microscopic mechanism of bond-deformation and breaking, we present below a first-principle strain-stress calculation, to further probe the mechanical properties of LiBC₁₁ and Li₂B₂C₁₀ under large structural deformations.

Table 3 The calculated elastic constants C_{ij} (GPa), bulk modulus B_0 (GPa), shear modulus G_0 (GPa), G_0/B_0 and Vickers hardness H_v of C₁₂, LiBC₁₁ and Li₂B₂C₁₀.

Structure	C_{11}	C_{22}	C_{33}	C_{44}	C_{55}	C_{66}	C_{12}	C_{13}	C_{23}	B_0	G_0	G_0/B_0	H_v
C ₁₂	797			300			102			334	319	0.955	51.5
LiBC ₁₁	727	732	631	253	246	268	94	115	106	302	271	0.895	48.8
Li ₂ B ₂ C ₁₀	676		676	209		209	156	87		282	232	0.824	37.7

The ideal strength, the maximum stress that a material can sustain, is the upper bound to the critical stress for crack formation and dislocation nucleation in the material. When the applied stress exceeds the ideal strength, the crystal structure will collapse even at zero temperature. Therefore, a strain-stress calculation also serves to describe the upper bound limit of the hardness of a material.

We have examined the stress-strain relations of LiBC_{11} and $\text{Li}_2\text{B}_2\text{C}_{10}$ under tensile loadings. The results are shown in Fig. 4 (upper panels). LiBC_{11} shows remarkably strong stress response in the $\langle 010 \rangle$ directions with the peak tensile stress reaching 110 GPa. The peak tensile stresses along the $\langle 001 \rangle$, $\langle 110 \rangle$, $\langle 100 \rangle$, $\langle 111 \rangle$, and $\langle 101 \rangle$ directions are also high, ranging from 62 GPa to 86 GPa. The lowest tensile strength, corresponding to the weakest direction, lies along the $\langle 011 \rangle$ direction and peaks at 49 GPa. Our results show that when the tensile stress exceeds 49 GPa, the $\{011\}$ type planes of the crystal first become unstable against cleavage fracture. For $\text{Li}_2\text{B}_2\text{C}_{10}$, the highest tensile strength is 99 GPa along the $\langle 100 \rangle$ directions, followed by 91 GPa along the $\langle 001 \rangle$ directions. The weakest tensile strength is along $\langle 101 \rangle$ type directions with a value of 49 GPa, indicating that $\text{Li}_2\text{B}_2\text{C}_{10}$ would fail by cleavage in the $\langle 101 \rangle$ direction at 49 GPa. Similar to the estimations from the empirical model, the conclusion that LiBC_{11} and $\text{Li}_2\text{B}_2\text{C}_{10}$ are both superhard is valid.

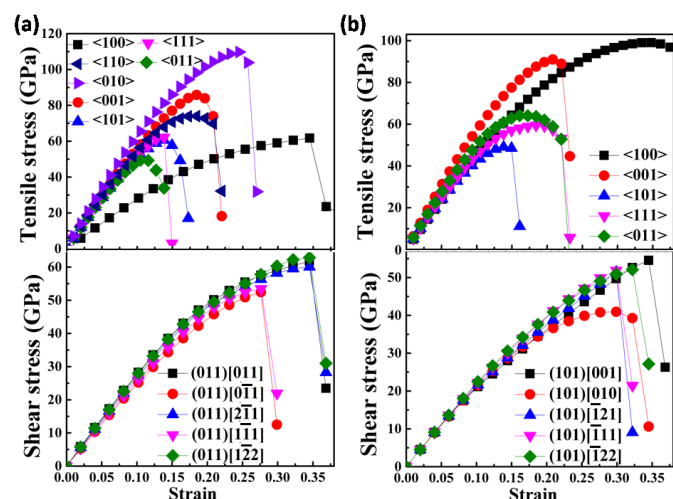


Fig. 4 (colour online) The calculated strain-stress relation in various tensile (upper panels) and shear (lower panels) directions of (a) LiBC_{11} and (b) $\text{Li}_2\text{B}_2\text{C}_{10}$ at 0 GPa, respectively.

We now turn to ideal shear strength in the tensile-weakest (easiest-cleavage) plane. Various non-equivalent directions along the shear-sliding planes have been systematically studied under shear deformations, as shown in Fig. 4 (lower panels). It can be seen that the shear strengths of LiBC_{11} range from 52 GPa to 63 GPa, with the weakest one being the $\langle 011 \rangle$ [011] shear system with the value of 49 GPa. Therefore, the resulting hardness of LiBC_{11} compound is calculated to be 49 GPa, which is in good agreement with the estimated value from the empirical microscopic hardness model (0.41%). For $\text{Li}_2\text{B}_2\text{C}_{10}$, the shear strengths fall over a narrow range from 53 GPa to 56 GPa for most of the shear directions, apart from $(101)[010]$ direction, along which the $\text{Li}_2\text{B}_2\text{C}_{10}$ crystal is unstable against slip on crystallographic planes when the shear stress exceeds 41 GPa. The lowest shear strength of 41 GPa is smaller than the ideal tensile strength, suggesting that the hardness of $\text{Li}_2\text{B}_2\text{C}_{10}$ is slightly lowered. Nevertheless, since the lowest shear

strength surpasses the threshold (40 GPa), it still can be classified as superhard materials.

Conclusion

Using first-principle calculations, we have investigated the structural, electronic, dynamical, and mechanical properties of two Li-doped B-substituted carbon cages: LiBC_{11} and $\text{Li}_2\text{B}_2\text{C}_{10}$. The electronic structures suggest that both compounds are semiconductors. Phonon dispersion and elastic constant calculations demonstrate that both are dynamically and mechanically stable at ambient condition. First-principles strain-stress relations at large strains were also computed to examine the structural and mechanical properties. The established ideal tensile strength of 49 GPa in the $\langle 011 \rangle$ direction and ideal shear strength of 41 GPa along $(101)[010]$ direction both suggest that LiBC_{11} and $\text{Li}_2\text{B}_2\text{C}_{10}$ may be regarded as superhard materials.

Acknowledgements

X. F. and Q. L. acknowledge the funding supports from the National Natural Science Foundation of China under Grant Nos. 11474125, 11274136 and 11534003. J. T. and H. L. acknowledge the National Science Foundation of China (11474126) and support from the University of Saskatchewan research computing group and the use of the HPC resources (Plato machine).

References

- J. Hao, H. Liu, W. Lei, X. Tang, J. Lu, D. Liu and Y. Li, *The Journal of Physical Chemistry C*, 2015, **119**, (51), 28614-28619.
- L. Yinwei, L. Quan and M. Yanming, *EPL (Europhysics Letters)*, 2011, **95**, (6), 66006.
- Q. Li, M. Wang, A. R. Oganov, T. Cui, Y. Ma and G. Zou, *Journal of Applied Physics*, 2009, **105**, (5), N.PAG.
- V. L. Solozhenko, D. Andrault, G. Fiquet, M. Mezouar and D. C. Rubie, *Applied Physics Letters*, 2001, **78**, (10), 1385.
- Q. Li, J. Wang, M. Zhang, Q. Li and Y. Ma, *RSC Advances*, 2015, **5**, (45), 35882-35887.
- H. Liu, Q. Li, L. Zhu and Y. Ma, *Physics Letters A*, 2011, **375**, (3), 771-774.
- M. Zhang, H. Liu, Q. Li, B. Gao, Y. Wang, H. Li, C. Chen and Y. Ma, *Physical Review Letters*, 2015, **114**, (1), 015502.
- L. Quan, W. Hui, T. Yongjun, X. Yang, C. Tian, H. Julong, M. Yanming and Z. Guangtian, *Journal of Applied Physics*, 2010, **108**, (2), 023507.
- V. L. Solozhenko, O. O. Kurakevych, D. Andrault, Y. Le Godec and M. Mezouar, *Physical Review Letters*, 2009, **102**, (1), 015506.
- H. Liu, Q. Li, L. Zhu and Y. Ma, *Solid State Communications*, 2011, **151**, (9), 716-719.
- M. Kobayashi, I. Higashi, C. Brodhag and F. Thevenot, *Journal of materials science*, 1993, **28**, (8), 2129-2134.
- X. Tang, J. Hao and Y. Li, *Physical Chemistry Chemical Physics*, 2015, **17**, (41), 27821-27825.
- Q. Li, H. Liu, D. Zhou, W. Zheng, Z. Wu and Y. Ma, *Physical Chemistry Chemical Physics*, 2012, **14**, (37), 13081-13087.
- Q. Li, M. Wang, A. R. Oganov, T. Cui, Y. Ma and G. Zou, *Journal of Applied Physics*, 2009, **105**, (5), 53514.
- Y. Zhang, H. Sun and C. Chen, *Physical review letters*, 2004, **93**, (19), 195504.
- R. Wentorf Jr, *The Journal of Chemical Physics*, 1957, **26**, (4), 956-956.
- Y. Li, J. Hao, H. Liu, S. Lu and J. S. Tse, *Physical Review Letters*, 2015, **115**, (10), 105502.
- T. Zeng, R. Hoffmann, R. Nesper, N. W. Ashcroft, T. A. Strobel and D. M. Proserpio, *Journal of the American Chemical Society*, 2015, **137**, (39), 12639-12652.

19. J. F. Ditter, E. B. Klusmann, J. D. Oakes and R. E. Williams, *Inorganic Chemistry*, 1970, **9**, (4), 889-892.
20. G. Kresse and J. Furthmüller, *Physical Review B*, 1996, **54**, (16), 11169-11186.
21. J. P. Perdew, K. Burke and M. Ernzerhof, *Physical Review Letters*, 1996, **77**, (18), 3865-3868.
22. G. Kresse and D. Joubert, *Physical Review B*, 1999, **59**, (3), 1758-1775.
23. H. J. Monkhorst and J. D. Pack, *Physical Review B*, 1976, **13**, (12), 5188-5192.
24. A. Togo and I. Tanaka, *Scripta Materialia*, 2015, **108**, 1-5.
25. A. Togo, F. Oba and I. Tanaka, *Physical Review B*, 2008, **78**, (13), 134106.
26. R. Hill, *Proceedings of the Physical Society. Section A*, 1952, **65**, (5), 349.
27. J. Tse, *Journal of Superhard Materials*, 2010, **32**, (3), 177-191.
28. Z. Pan, H. Sun and C. Chen, *Physical Review Letters*, 2007, **98**, (13), 135505.
29. Z. Pan, H. Sun, Y. Zhang and C. Chen, *Physical Review Letters*, 2009, **102**, (5), 055503.
30. K.-W. Sun, Y.-Y. Zhang and Q.-H. Chen, *Physical Review B*, 2009, **79**, (10), 104429.
31. Y. Zhang, H. Sun and C. Chen, *Physical Review Letters*, 2004, **93**, (19), 195504.
32. F. J. Ribeiro, P. Tangney, S. G. Louie and M. L. Cohen, *Physical Review B*, 2006, **74**, (17), 172101.
33. B. Wong and J. Cordaro, *The Journal of Physical Chemistry C*, 2011, **115**, (37), 18333-18341.
34. B. Janesko, *J. Chem. Phys.*, 2011, **134**, 184105.
35. A. El Goresy, L. S. Dubrovinsky, P. Gillet, S. Mostefaoui, G. Graup, M. Drakopoulos, A. S. Simionovici, V. Swamy and V. L. Masaitis, *Comptes Rendus Geoscience*, 2003, **335**, (12), 889-898.
36. J. F. Nye, *Physical properties of crystals: their representation by tensors and matrices*. (Oxford university press, 1985).